J. Inst. Eng. India Ser. C (October–December 2014) 95(4):309–318
DOI 10.1007/s40032-014-0129-x

ORIGINAL CONTRIBUTION

Transient Analysis of Ball Bearing Fault Simulation using Finite Element Method

S. Tyagi · S. K. Panigrahi

Received: 19 February 2014 / Accepted: 4 July 2014 / Published online: 10 August 2014

Abstract Effectiveness of transient analysis of the finite element bearing model to simulate the vibration signal emanating from ball bearing with faults is presented in this work. It is difficult to identify the ball bearing defect either in frequency spectrum or time domain when the defect is at incipient stage. Further, it is difficult to experimentally obtain vibration signals from bearing having fault at incipient stage. Thus, need for accurate simulation of ball bearing fault at incipient stage is considered essential. A Computer Aided Design (CAD) model of a ball bearing having a minor crack in outer-race was created using commercially available software. It was shown that identification of ball bearing defect in frequency spectrum is difficult. The results were validated with experimental results.

Keywords Rolling element bearing · Vibration analysis · Transient analysis · Finite element method (FEM)

Introduction

Rolling Element Bearings (REB) are the most common machine elements used in rotating machinery and their failure is the foremost cause of down time in plant machinery [1].

Commonly occurring REB defects are cracks and pits located at outer race, inner race and on the rolling element [2]. These defects generate a sequence of impacts with each passage of rolling element over the defect due to the metal to metal contact [3]. The ensuing vibration is distinguished by sharp peaks. It is not easy to identify the defect frequency in the spectrum as these impact vibrations disseminate their energy over broad range of frequencies, thus the bearing's defect frequency contains low energy [4] and hence can be easily masked by noise and other low frequency effects.

To overcome this problem, both time and frequency domain methods have been developed [5, 6]. Time domain methods usually involve indices that are sensitive to impulsive oscillations, such as peak level, Root Mean Square (RMS) value, crest factor analysis, kurtosis and shock pulse counting [7–10]. Since it is difficult to identify incipient bearing defects in the frequency spectrum [11], many specialised techniques have been developed over the years for bearing fault diagnosis, such as, Bi-spectrum coherence [12], spectral entropy [13], autoregressive models [14], envelope spectrum [15] wavelet transform [16] and more Artificial Neural Network (ANN) [17] to machinery fault diagnosis. In practice, it is quite difficult to obtain vibration signal from bearing having incipient defects [18]; thus many researchers have attempted to simulate the vibration signal emanating from bearing having incipient fault [19, 20].

In the present work, a method to simulate the ball bearing having an incipient crack on outer race has been presented. Transient analysis of the bearing was performed and nodal acceleration of a node on a region on outer race that was not constrained was recorded with respect to time. The results of transient analysis was compared with actual vibration signals emanating from ball bearing embedded with induced fault (crack) on outer race vibration data of a rotating shaft-line. It was shown that simulated signal matches with the actual vibration signal and it was also

S. Tyagi · S. K. Panigrahi (✉)
Department of Mechanical Engineering, Defence Institute of Advance Technology, Pune, Maharashtra 411025, India
e-mail: panigrahi.sk@gmail.com

shown that identification of bearing faults at incipient stage is not very evident in time domain or in frequency domain. It was also shown that more accurate simulation is achieved when Finite Element (FE) model of full bearing assembly is done instead of making FE model of only outer-race or inner-race as done by various researchers [21].

Rolling Element Bearing Defects

Common Defect Types

Most common REB defects are cracks or pits located at outer race, inner race and on the rolling element as shown in Fig. 1.

Rolling bearings consist of two concentric rings, called the inner raceway and outer raceway, with a set of rolling elements running in their tracks. Since most bearing rotations are periodical, hence, it is easy to calculate characteristic frequency of defect.

Typically, the rolling elements in a bearing are guided in a cage that ensures uniform spacing and prevents mutual contact. The dynamics of bearing elements can be described by five basic motions such as the shaft rotational frequency, the fundamental cage frequency, the ball pass inner raceway frequency, the ball pass outer raceway frequency, and the ball rotational frequency, with each movement having a corresponding frequency.

Bearing Frequencies

The five basic motions of the rolling element bearing and their corresponding frequencies are depicted in Fig. 2. Most significant frequencies are:

(a) Shaft Rotational Frequency (F_s): As bearings are often used to form a bearing–rotor system, the speed of the rotor (or shaft), F_s, is the most important movement of bearings. All other frequencies are a function of this frequency.

(b) Fundamental Cage Frequency (F_c): The fundamental cage frequency, F_c, is the rotational speed of the cage (cage frequency). It can be derived from the linear velocity of a point on the cage, which is the mean of the linear velocities of the inner raceway and the outer raceway.

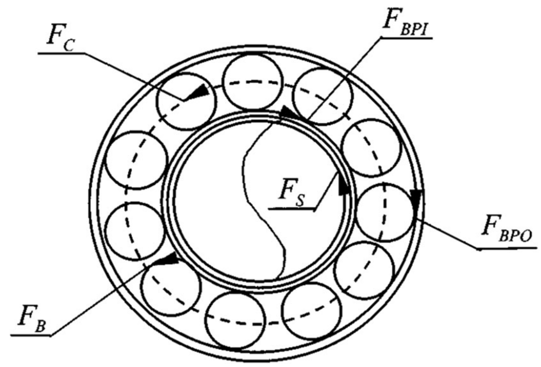

Fig. 2 Frequencies of five basic motions of bearing

(c) Ball Pass Raceway Frequencies (F_{BPO} *and* F_{BPI}): These frequencies pertain to the rate at which the balls of the ball-bearing would pass over a groove in outer raceway (F_{BPO}) and a groove in inner raceway (F_{BPI}). Both these frequencies are the functions of the number of balls in a bearing, shaft rotational frequency and fundamental cage frequency.

(d) Ball Pass Frequency Rolling Element (F_B): This pertains to the rate at which a point (or a pit) on a rolling element (ball) of a ball-bearing would touch the inner and outer raceways. Ball Pass Frequency Rolling Element (F_B) is a function of the number of balls in a bearing, shaft rotational frequency, ball and pitch diameter.

The bearing characteristic frequencies are calculated from the geometric parameters of the bearing, number of balls and shaft frequency as given below:

$$F_c = \frac{F_s}{2}\left(1 - \frac{B_d}{P_d}\cos\emptyset\right) \tag{1}$$

$$F_{BPO} = \frac{z}{2}\,F_s\left(1 + \frac{B_d}{P_d}\cos\emptyset\right) \tag{2}$$

$$F_{BPI} = \frac{z}{2}\,F_s\left(1 - \frac{B_d}{P_d}\cos\emptyset\right) \tag{3}$$

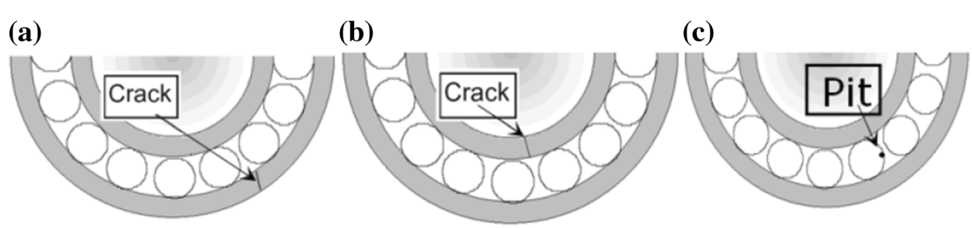

Fig. 1 Bearing defects **a** outer race fault. **b** Inner race fault. **c** Ball fault

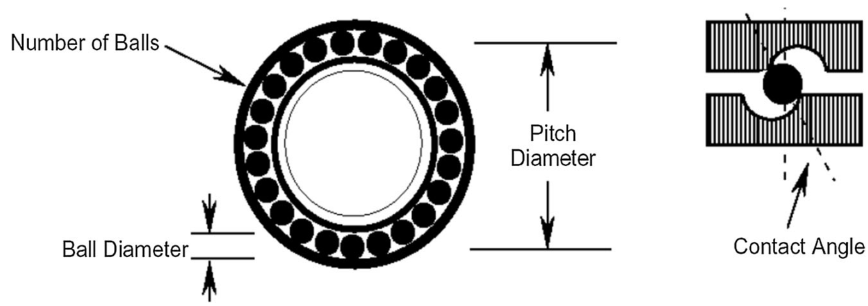

Fig. 3 Basic dimensions of ball bearing

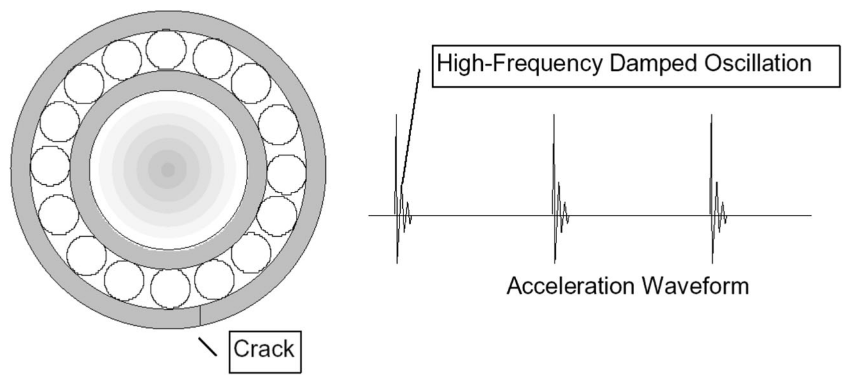

Fig. 4 Typical time domain vibration signal of bearing with outer race defect

$$F_B = \frac{z}{2}\ F_s\left(1 - \left(\frac{B_d}{P_d}\right)^2 \cos\emptyset\right) \tag{4}$$

where B_d is the ball diameter, P_d is the pitch diameter, Z is the number of balls, F is the shaft rotation frequency and φ is the contact angle (Fig. 3).

Vibration Signal of Rolling Element Bearing Defects

Bearing defect generates a series of impacts to which bearing response is a high frequency damped oscillation. These impacts occur periodically at bearing characteristic (defect) frequency, which is calculated from the geometry of bearing, shaft speed and type of defect. These defects generate a series of impacts as rolling element passes over the defect due to the metal to metal contact. The resultant vibration is characterised by sharp peaks in time domain signal (Fig. 4). It is difficult to identify the defect frequency in spectrum as these impact vibrations distribute their energy over wide range of frequencies; the defect frequency of the bearing contains low energy and hence can be easily masked by noise and other low frequency effects. The frequency of occurrence of the impacts is the bearing characteristic defect frequency. These impacts excite the bearing structural resonant frequency. The response is a periodic burst of exponentially decaying high frequency oscillations (the bearing structural resonant frequency). The oscillations are of extremely short duration compared to interval between impulses, thus it is difficult to detect them in conventional frequency spectrum [11].

Load Distribution

The loads carried by the ball and roller bearings are transmitted through the rolling elements from one ring to the other. As mentioned in [22], the relationship between load and deformation is:

$$Q = k\delta^n \tag{5}$$

where $n = 1.5$ for ball bearings and $n = 1.11$ for roller bearings, Q is the ball or roller normal load, δ is the deformation, and k is the load-deflection factor.

For a rigidly supported bearing subjected to radial load, the radial deflection (δ_ψ) at any rolling element angular position (ψ) is given by:

$$\delta_\psi = \delta_r \cos\psi - \frac{1}{2}P_d \tag{6}$$

in which δ_r is the ring radial shift, occurring at $\psi = 0$ and P_d is the diametrical clearance. Eq. 5 may be rearranged in terms of maximum deformation as follows:

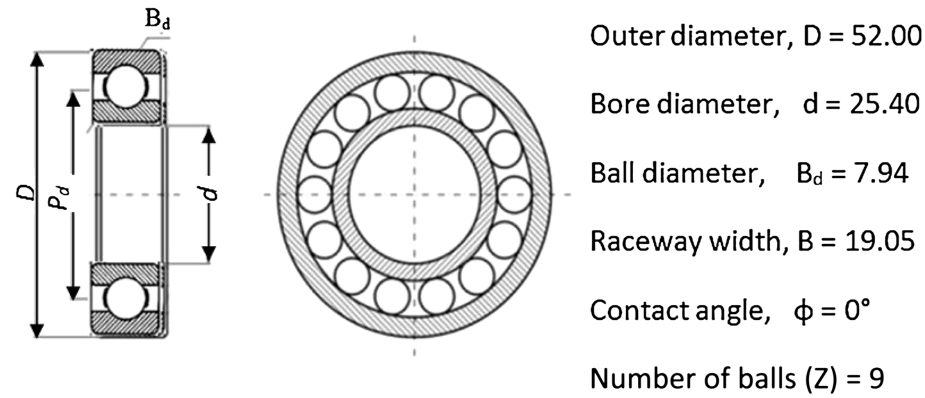

Fig. 5 Rexnord ER 16 K bearing geometry

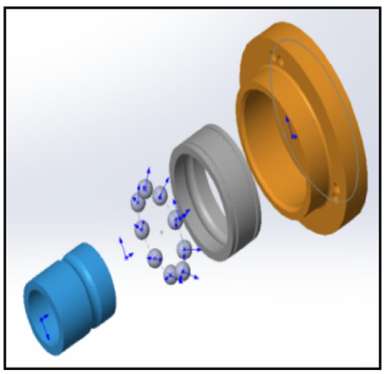

Fig. 6 CAD model exploded view

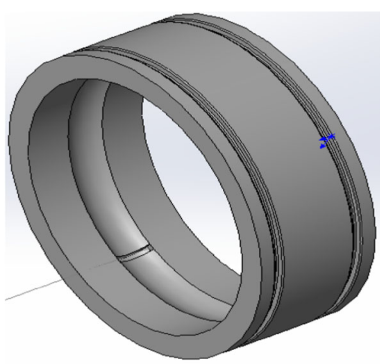

Fig. 7 Outer race with crack defect

$$\delta_\psi = \delta_{\max}\left[1 - \frac{1}{2\varepsilon}(1 - \cos\psi)\right] \tag{7}$$

where ε is the load distribution factor given by:

$$\varepsilon = \frac{1}{2}\left(1 - \frac{P_d}{2\delta_r}\right) \tag{8}$$

Thus, for ball bearings under pure radial load and zero clearance, we get the well-known Stribeck's Eqn [23]:

$$Q_{\max} = \frac{4.37F_r}{Z\cos\emptyset} \tag{9}$$

Structural Transient Analysis

A structural transient analysis is a FE analysis that determines the dynamic behaviour of a structure or component under arbitrary load. It is an analysis involving time, where apart from mass, stiffness and displacement, inertia and damping of the structure is also taken into account. The governing equation in matrix form for structural transient analysis is given in Eq. 9.

$$[M]\{\ddot{u}\} + [C]\{\dot{u}\} + [K]\{u\} = \{F\}, \tag{10}$$

where [M] is the structural mass matrix, [C] is the structural damping matrix, [K] is the structural stiffness matrix, $\{\ddot{u}\}$ is the nodal acceleration vector, $\{\dot{u}\}$ is the nodal velocity vector, $\{u\text{-}\}$ is the nodal displacement vector, $\{F\}$ is the applied load vector.

Nonlinearities, such as large deflections, nonlinear contact, material nonlinearities etc., are possible in a transient analysis. The external force {F} can be time dependent [24].

Simulation of Ball Bearing Defect

CAD Model of Bearing with Defect

To monitor the condition of a bearing, Rexnord ER 16 K ball bearing is used in this study. Figure 5 shows the geometry and dimensions of bearing. Figure 6 shows the CAD model of the bearing with bearing casing.

A slit 0.5 mm wide and 0.5 mm deep spanning horizontally across raceway on outer-race was created to simulate defect on outer-race as shown in Fig. 7.

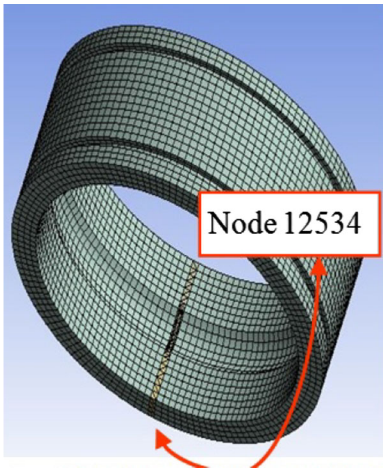

Fig. 8 Outer race after meshing

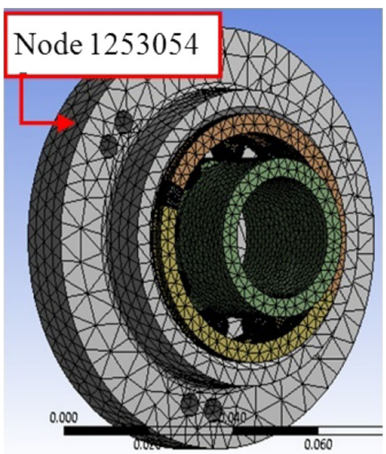

Fig. 9 Complete bearing assembly after meshing

Transient Analysis of FE Model of Bearing Defect

Initially a FE model was created by taking into account only the outer race (as shown in Fig. 8) as was done by various researchers in the past [21]. As depicted in Fig. 8, the outer race structure of the bearing was partitioned in three parts to enable finer mesh around the defect zone. The dynamic response of node 12534 was obtained for analysis.

The housing structure was discretised using 20-noded hexahedron (brick) finite elements. The material of both bearing and its housing was considered to be isotropic (Alloy Steel) with properties as, $E = 207$ GPa, $\mu = 0.3$, $\rho = 7{,}860$ kg/m^3. The researchers have [25] advocated the use of hexahedron (brick) elements with 20 nodes in cases where geometry is uneven and where there is irregular distribution of radial and circular stresses. Thus 20-noded hexahedron (brick) finite elements were employed in the present research in order to achieve better results closer to the analytical solution.

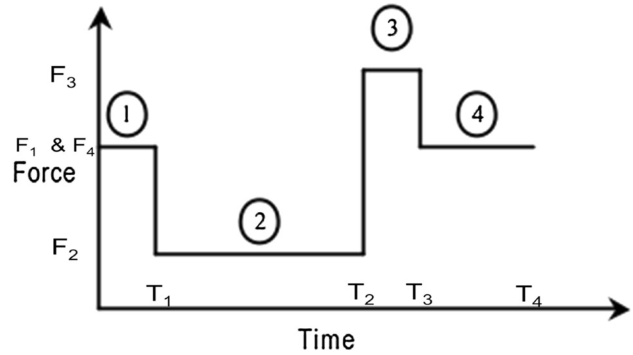

Fig. 10 Load steps for transient analysis

With a view to achieve better simulation; the FE model of the complete bearing assembly i.e. outer-race, inner-race, rolling elements and bearing housing was created as shown in Fig. 9.

Application of Load

Transient analysis of the meshed model was conducted. The outer race was assumed to be stationary and the defect zone was placed at the bottom. Frictional constraint was applied between the outer-race and casing. Fixed constraints were applied at the location of casing securing studs. Frictionless constraints were applied at contacts of balls with inner and outer races. In normal operation, the load of the bearing is supported by all of the rolling elements in the load zone of the bearing. The radial force on the bearing was assumed to be 65.4 N which is the basic load rating of the bearing at 1,200 rpm (20 Hz). The value of $Q_{\max}$ was calculated using Eq. 8.

Thus for $F_r = 65.4$ N and $Z = 9$, the value for $q_{\max}$ was calculated as 21.5 N. This is the maximum force exerted on the outer race by a rolling element. Variation in the force exerted by the rolling element on the outer ring is seen when the rolling element passes over a defect. As the rolling element enters the defect, the force exerted tends to lessen in magnitude for as long as the rolling element is in the defect. When it impacts the other end of the defect, a surge in the force is seen because of the impact and then it reduces to the value of the force exerted by the rolling element on the outer ring during normal operating conditions [8] as shown in Fig. 10.

The simulation for both FE models was carried out for a ball strike on outer-race with shaft running speed of 1,200 rpm (20 Hz). The ball pass frequency outer race (BPO) is calculated using Eq. 1. For F = 20 Hz, the BPO is 71.44 Hz. Thus, the unit time taken for the entire simulation is equal to 1/BPO = 1/71.44 and it works out to be 1.399×10^{-2} s. The load steps for one pulse are as shown in Table 1.

Table 1 Load steps for one impact

Step	Load, (N)	Time step, (s)
1	31.5	$T1 = 3.4975 \times 10^{-3}$
2	21.5	$T2 = 9.4925 \times 10^{-3}$
3	34.5	$T3 = 1.049 \times 10^{-2}$
4	31.5	$T4 = 1.399 \times 10^{-2}$

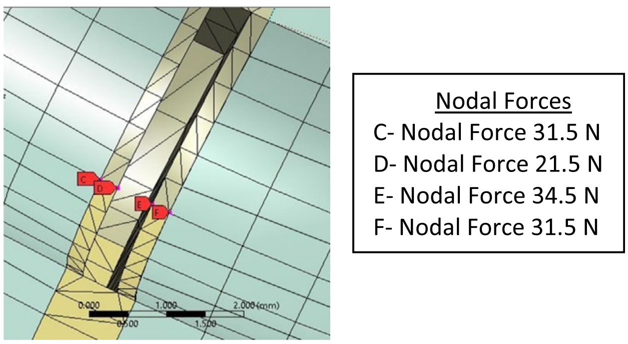

Fig. 11 Force exerted by rolling element on outer race

Location and variation in magnitude of force exerted by the rolling element on the outer ring as the rolling element passes over a defect are shown in Fig. 11.

Generation of Simulation and Analysis

Vibration response of a node 1253054 (on the bearing casing beneath defect zone on the outer race as shown in Fig. 9) was obtained by carrying out the transient analysis using ANSYS workbench and the solution was obtained in terms of Y component of acceleration for nine strikes of the ball on the defect on outer-race for nine strikes of ball. The signal was normalized so as to compare it with actual experimental signals without magnitude mismatch. Standard score formula [26] as given in Eq. 10 was used to normalize the signal.

$$S_n = \frac{(S_i - \mu)}{\sigma} \tag{11}$$

where S_i is the signal, μ represents the expectation of the signal, σ is the standard deviation and S_n is the normalized signal.

The normalized simulated signal for FE model of complete bearing is shown in Fig. 12a. Time Domain analysis of the generated acceleration signal reveals that there are impulses at regular intervals that are followed by high frequency damped oscillations as shown in Fig. 12b, the same effect was reported by the researchers [4]. These

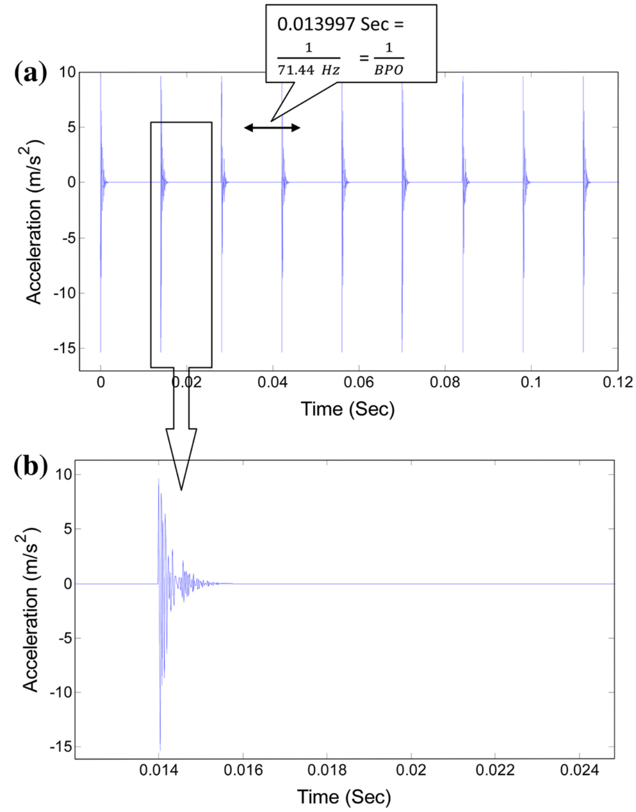

Fig. 12 **a** Simulated signal for nine strikes. **b** Zoomed view

impulses indicate the impact generated due to hitting of the rolling element on outer race surface crack as they passed over the defect and were damped due to inherent damping present in the structure. Reciprocal of time difference between two successive impulses were taken and the same indicated BPO.

The Fast Fourier Transform (FFT) of simulated time domain signal was obtained using a MATLAB code to analyse the simulated signal in frequency domain. Fig. 13a indicates the spectrum of bearing acceleration signal. High frequency component around 12, 18 and 24 kHz were predominant indicating possible resonance of some of the bearing components as indicated by the earlier investigators [3]. A zoomed view of spectrum up to 400 Hz is shown in Fig. 13b. This limit is chosen as ball pass frequency outer race (BPO = 71.4 Hz) and its first five harmonics are likely to be <400 Hz. A peak (although small) at BPO along with its multiples can be observed in the zoomed view of spectrum shown in Fig. 13b. The problem faced with the identification of bearing fault using frequency domain is that the peak at BPO is very small compared to other peaks in spectrum, hence it becomes difficult to identify the defect frequency [20].

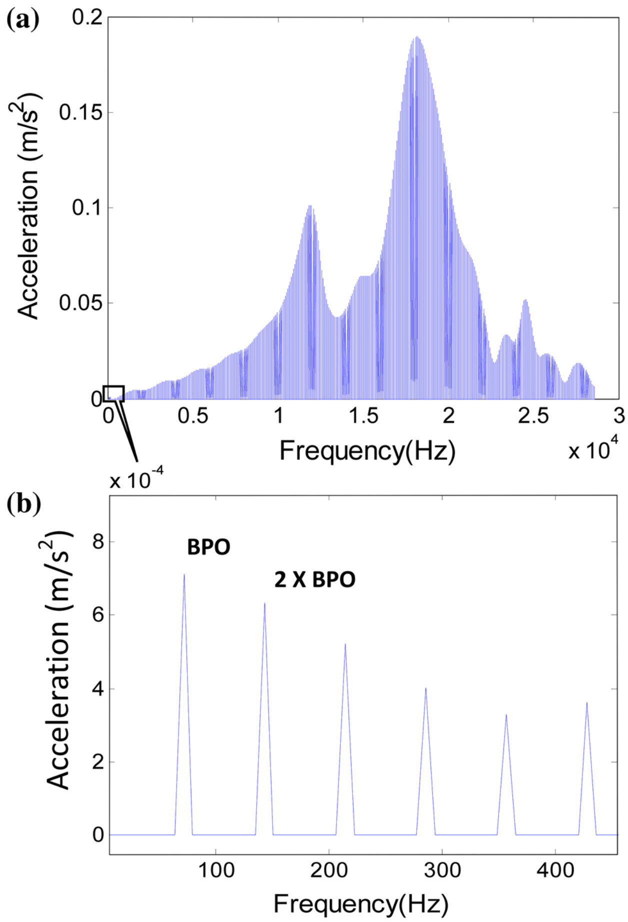

Fig. 13 **a** Spectrum of simulated signal. **b** Zoomed view

Experimental Setup

The test rig shown in Fig. 14 comprises of a variable speed AC motor driving main shaft of gearbox through flexible couplers. The shaft is rested on two ball bearings. A magnetic break is used to provide mechanical load to the setup. The bearings used were Rexnord type ER 16 K for which simulation was done. The vibration signal (acceleration) obtained from the accelerometer placed at bearing located at the drive end side was used for comparison with the simulated signal. Piezoelectric accelerometer type 4,347 of Bruel and Kjaer make with charge amplifier was used in the experimental setup. The accelerometer was stud mounted. The data was collected using a personal computer with Windows OS using 'OROS' data acquisition hardware and NV Gate software. Sampling frequency of 51.2 kHz was used. The outer race fault of approximate size of 0.5 mm width and 0.4 mm depth was artificially introduced in the bearing outer race by Electric Spark Erosion (ESE).

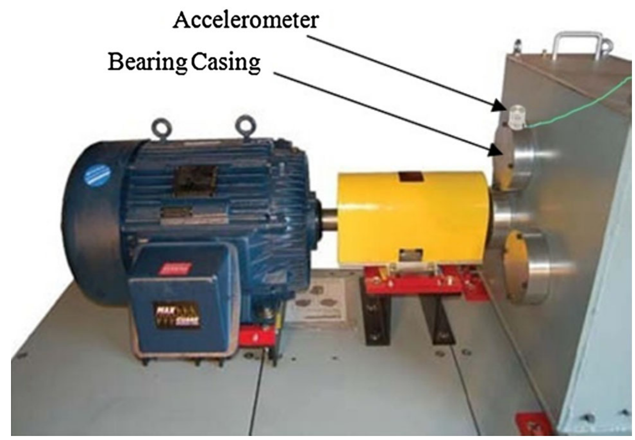

Fig. 14 The experimental setup

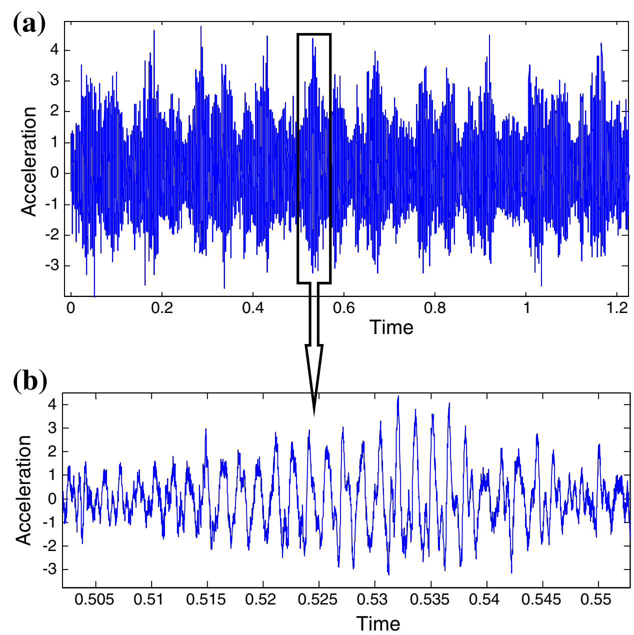

Fig. 15 **a** Experimental vibration signal. **b** Zoomed view

Experimental Results

The experiment was conducted with shaft line resting on bearing with outer race faults. The shaft was made to rotate at 1,200 rpm (20 Hz). The signal acquired in time domain (with accelerometer placed on bearing casing) is shown in Fig. 15.

The analysis of the experimentally obtained time domain signal shown in Fig. 15 reveals the presence of impulses and subsequent high frequency damped oscillation similar to those obtained in the simulated signal (Fig. 12). However, these impulses in actual signal are not as regular as obtained in simulated signal, possibly due to presence of many rotating and mating components in the gearbox.

Table 2 Statistical parameters

Signal	Parameter		
	RMS	Crest factor	Kurtosis
Simulated	0.999	13	8.8
Experimental	1	11	3.4

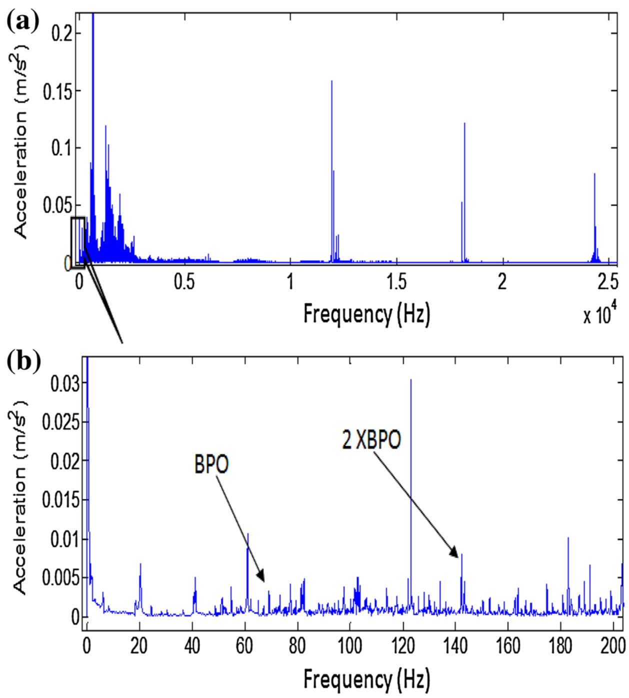

Fig. 16 **a** Spectrum of experimental signal. **b** Zoomed view

Table 2 presents the statistical parameters of the simulated and actual signals. The parameters selected are those that are referred to identify bearing faults [2]. The similarity of signals is also evident in these parameters. The crest factor is calculated as peak value divided by RMS and the Kurtosis is the fourth statistical moment. These parameters indicated the presence of bearing fault as crest factor beyond 3.5 and Kurtosis more than 4, which are indicative of bearing fault [2].

The FFT of actual (experimental) vibration signal obtained from experiment is shown in Fig. 16a, its resemblance can also be traced with the FFT of simulated signal of the FE model of complete bearing shown in Fig. 13a. The dominant peaks at about 12, 18 and 24 kHz are evident in both the cases. These are indicative of structural resonance of bearing components.

In case of incipient faults identification of bearing fault by spectrum analysis is rather difficult as the peak at BPO is not very distinct and its harmonics are even more difficult to detect [2]. In the zoomed view of the spectrum of experimental signal shown in Fig. 16b; a peak at BPO

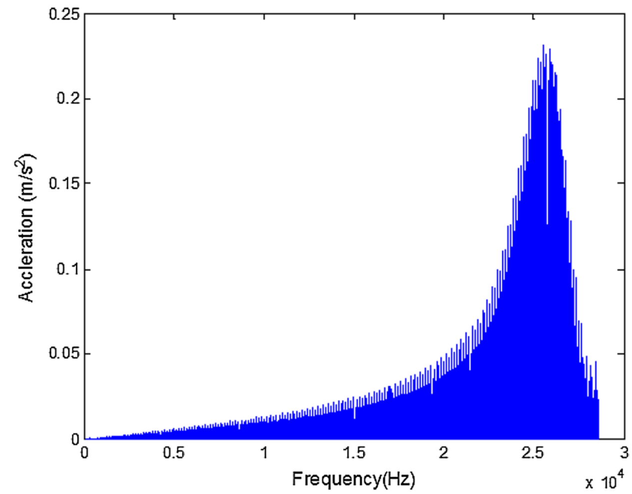

Fig. 17 Transient response spectrum of FE model with only outer-race

(71.44 Hz) and its second harmonic (2 X BPO) are visible but these were very small compared to other prominent peaks in the spectrum and are, thus, difficult to detect and monitor. However, similarity of experimental signal with simulated signal can also be seen in zoomed views of the spectrums of both simulated and experimental signal as peaks at BPO and its second harmonic are seen in both cases.

For FE model when only outer race was modelled (Fig. 9) the FFT of its transient response (of node 12534) is shown in Fig. 17. It can be deduced from the plot that this simulation is not accurate; as the spectrum obtained is quite different than that of the actual experimental signal. The spectrum in Fig. 17 shows only one peak at 24 kHz whereas the spectrum of experimental signal (Fig. 16a) displayed three distinct peaks in resonant zone (i.e. frequency more than 10 kHz). Comparison of spectrums of both the simulations shown in Figs. 14a and 17 with that of FFT of the experimental signal (Fig. 16a) demonstrates that simulation made with FE model considering all bearing components (Fig. 14a) is more accurate than FE simulation with only outer race (Fig. 17) as three peaks at 12, 18 and 24 kHz in Fig. 14a can be seen which is similar to that of the experimental spectrum.

Conclusion

In this study, the FE model of a bearing with a minor crack outer race has been developed using the commercial CAD and FEM software. Also, a method for dynamic loading distribution is developed to simulate the load distribution on the outer raceway due to load transfer from the shaft through the balls. The impulse force due to impact between the defect and the bearing components is presented by reducing the excitation force while the ball is over the defect and amplifying the excitation force as the ball hits the other end of the crack. Two FE models were developed; one model was a simplified version that considered only the outer-race of ball bearing while the other considered all components of ball bearings. Transient analyses of both the models were performed to obtain the vibration signal in the time and frequency domains. Experiments were conducted to validate the simulation results. It was found that the simulation and experimental results are in good agreement with each other. It was found that more accurate simulation is achieved when ball bearing was simulated with all components of the bearing.

It was also found that for incipient defect; identification of bearing faults is quite difficult through spectrum analysis. The peak at bearing defect frequency is quite small in comparison to other peaks in the spectrum. The transient analysis of FE model of bearing is a powerful method for bearing defect simulation since signals of experimental result and simulation matched with each other in the time domain as well as in frequency domain spectrums matched with each other.

Acknowledgments This paper is a revised and expanded version of an article entitled, ''Simulation of Ball Bearing Defect using Finite Element Transient Analysis'' presented in ''National Conference on Recent Advancements in Mechanical Engineering'' held at 'North East Regional Institute of Science and Technology', Arunachal Pradesh, India during November 8–9, 2013.

References

1. E. Mendel, T.W. Rauber, F.M. Varejao R.J. Batista, Rolling element bearing fault diagnosis in rotating machines of oil extraction rigs. 17th european signal processing conference (EUSIPCO 2009), Glasgow, Scotland, August 24–28, 2009, pp. 1602–1606
2. M.P. Norton, *Fundamentals of Noise and Vibration Analysis for Engineers*, 1st edn edn. (Cambridge University Press, Cambridge, 1989), pp. 518–554. ISBN ISBN 0-521-34941-9
3. J. Pineyro, A. Klempnow, V. Lescano, Effectiveness of new spectral techniques in the anomaly detection of rolling element bearings. J. Alloy. Compd. **310**, 276–279 (2000)
4. N. Tandon, A. Choudhury, A review of vibration and acoustic measurement methods for the detection of defects in rolling element bearings. Tribol. Int. **32**, 469–480 (1999)
5. T. Miyachi K. Seki, An investigation of early detection of defects in ball bearings using vibration monitoring–practical limit of detectability, in *Proceedings of the International Conference on Rotodynamics, JSME-IFToMM,* Tokyo, 14-17 September, 1986, pp. 403–408
6. F.D. Lorenzo, M. Calabro, Kurtosis: a statistical method to identify defect in rolling element bearings, in *2nd International Conference on Marine Research and Transport*, Napels, Italy, 28–30 June 2007, pp. 17–24
7. M. Yadav, S. Wadhwani, Vibration analysis of bearing for fault detection using time domain features and neural network. Internatl. J. Appl. Res. Mech. Eng **1**(1), 69–74 (2011)
8. S. Goreczk, J. Strackeljan, Optimization of time domain features for rolling bearing fault diagnostics, in *The 6th International Conference on Condition Monitoring and Machinery Failure Prevention Technologies*, Dublin, Ireland 23–25 June, 2009, pp 642–652
9. J. Chebil, G. Noel, M. Mesbah, M. Deriche, Wavelet decomposition for the detection and diagnosis of faults in rolling element bearings. Jordan J. Mech. Ind. Eng. **3**, 260–267 (2009)
10. B. Sreejith, A.K. Verma, A. Srividya, Fault diagnosis of rolling element bearing using time-domain features and neural networks. in *The 3rd International Conference on Industrial & Information Systems*, Kharagpur, India, 8–10 December 2008
11. Y.T. Su, Y.T. Sheen, On the detectability of roller bearing damage by frequency analysis, in *Proceedings of the Institution of Mechanical Engineers*, Part C: J. Mech. Eng. Sci., vol. 207, No. 1, January 1993, pp. 23–32
12. C.J. Li, J. Ma, B. Hwang, Bearing condition monitoring by pattern recognition based on bicoherence analysis of vibrations, in *Proceedings of the Institution of Mechanical Engineers,* Part C: J. Mech. Eng. Sci. vol. 210, No. 3, May 1996, pp. 277–285
13. Y.N. Pan, J. Chen, X.L. Li, Spectral entropy: a complementary index for rolling element bearing performance degradation assessment, in *Proceedings of the Institution of Mechanical Engineers*, Part C: J. Mech. Eng. Sci. vol. 223, No. 5, May 1, 2009, pp. 1223–1231
14. A.C. McCormick, A.K. Nandi, L.B. Jack, Application of periodic time-varying autoregressive models to the detection of bearing faults, in *Proceedings of the Institution of Mechanical Engineers*, Part C: J. Mech. Eng. Sci. vol. 212 No. 6, June 1, 1998, pp. 417–428
15. R. Jiang, J. Chen, G. Dong, T. Liu, W. Xiao, The weak fault diagnosis and condition monitoring of rolling element bearing using minimum entropy deconvolution and envelop spectrum, in *Proceedings of the Institution of Mechanical Engineers*, Part C: J Mech Eng Science vol. 227 No. 5, May 2013, pp. 1116–1129
16. P.W. Tsea, W. Yangb, H.Y. Tama, Machine fault diagnosis through an effective exact wavelet analysis. J. Sound Vib. **277**, 1005–1024 (2004)
17. I.E. Alguindigue, A. Loskiewicz-Buczak, R.E. Uhrig, Monitoring and diagnosis of rolling element bearings using artificial neural networks. IEEE Trans. Industr. Electron. **40**(2), 209–217 (1993)
18. S. Tyagi, A comparative study of SVM classifiers and artificial neural networks application for rolling element bearing fault diagnosis using wavelet transform pre-processing. J. World Acad. Sci. Eng. Tech. **43**, 309–317 (2008)
19. Z. Taha, N.T. Dung, Rolling element bearing fault detection with a single point defect on the outer raceway using finite element analysis. in *The 11th Asia Pacific Industrial Engineering and Management Systems Conference*, Melaka, Malaysia, Dec 2010, 7–10
20. M. Tadina, M.B. Zar, Improved model of a ball bearing for the simulation of vibration signals due to faults during run-up. J. Sound Vib. **300**(17), 4287–4301 (2011)
21. L.G. Deshpande, N.M. Sawalhi, R.B. Randall, Bearing fault simulation using finite element model updating and reduction techniques, in *Proceedings of the 7th Australasian Congress on Applied Mechanics* (ACAM 7), Barton, ACT, Australia, 9–12 December 2012, pp. 148-154
22. T.A. Harris, M.N. Kotzalas, *Rolling Bearing Analysis*, 5th edn. edn. (CRC Press, Boca Raton, 2006)
23. A.S. Malhi, Finite element modeling of vibrations caused by a defect in the outer ring of a ball bearing. Project Report finite element method and applications, MIE 605, University of Massachusetts, 2002, pp. 1–6

24. H.H. Lee, *Finite Element Simulation with ANSYS Workbench 14 Theory Applications and Case Studies* (SDC Publications, Kansas, 2012)
25. M. Jovanović, P. Milić, D. Janošević, G. Petrović, Accuracy of the FEM analyses in the function of the finite element type selection. Facta Univ. Ser. Mech. Eng. **8**(1), 1–8 (2010)
26. R.J. Larsen, M.L. Marx, *An Introduction to Mathematical Statistics and its Applications*, 3rd edn. edn., 2000, pp. 282–283